Trends in Medical Research

ISSN 1819-3587

Academic Journals Inc.

www.academicjournals.com

OPEN ACCESS Trends in Medical Research

ISSN 1819-3587
DOI: 10.3923/tmr.2017.1.13

Research Article
Topical Temperature-sensitive Gel Containing DsiRNA-chitosan Nanoparticles for Potential Treatment of Skin Cancer

Haliza Katas, Teh Thian Siang and Maria Abdul Ghafoor Raja

Centre for Drug Delivery Research, Faculty of Pharmacy, Universiti Kebangsaan Malaysia, Jalan Raja Muda Abdul Aziz, 50300 Kuala Lumpur, Malaysia

Abstract

Background: Target specific delivery of RNA interference (RNAi)-based molecules against Vascular Endothelium Growth Factor (VEGF) has been regarded as a promising approach in skin cancer therapy like melanoma. Chitosan (CS) nanoparticles have been extensively studied for efficient delivery of RNAi-based molecules such as small interfering RNA (siRNA) and Dicer-substrate RNA (DsiRNA). **Materials and Methods:** The CS nanoparticles were prepared via ionic gelation method prior to DsiRNA adsorption. The DsiRNA-loaded CS nanoparticles were later incorporated into PF-127 (25 and 30% w/v) to form temperature-sensitive gels to facilitate their delivery through the skin barrier. The gels were later subject to rheology, FTIR, scanning electron microscopy analysis and gelation temperature as well as drug release determination. **Results:** Particle size of the resultant DsiRNA-loaded CS nanoparticles ranged from 146.0±19.3 to 217.7±20.5 nm with variable encapsulation efficiency (81.8±1.8 to 90.1±1.8%), depending on CS concentration. The gel (PF-127 25% w/v) containing DsiRNA-loaded CS nanoparticles had the desired viscosity (0.751±0.005 to 0.839±0.04 Pa sec) as well as gelation temperature (24.3±0.6 to 25.3±0.6) and exhibited a sustained drug release for almost 7 days. **Conclusion:** A temperature-sensitive gel containing DsiRNA-loaded CS nanoparticles was successfully developed and it has a potential to be further developed as a gene delivery system for skin cancer therapy.

Key words: Drug delivery system, pluronic, ionic gelation, topical gel, biodegradable polymer

Received: July 14, 2016 Accepted: October 05, 2016 Published: December 15, 2016

Citation: Haliza Katas, Teh Thian Siang and Maria Abdul Ghafoor Raja, 2017. Topical temperature-sensitive gel containing DsiRNA-chitosan nanoparticles for potential treatment of skin cancer. Trends Med. Res., 12: 1-13.

Corresponding Author: Haliza Katas, Centre for Drug Delivery Research, Faculty of Pharmacy, Universiti Kebangsaan Malaysia, Kuala Lumpur Campus, Jalan Raja Muda Abdul Aziz, 50300 Kuala Lumpur, Malaysia Tel:+60392897971 Fax:+60326983271

Competing Interest: The authors have declared that no competing interest exists.

Data Availability: All relevant data are within the paper and its supporting information files.

INTRODUCTION

Angiogenesis is an essential step for cancer development and has been recognised as a hallmark of cancers[1]. Vascular Endothelium Growth Factor (VEGF) is the most described secreted molecules implicated in angiogenesis of human cancers[2]. Numerous inhibitors have been developed to slow down angiogenesis. These include RNA interference (RNAi)-based therapy for example, small interfering RNA (siRNA) and a more potent molecule, Dicer-substrate RNA (DsiRNA). The DsiRNA demonstrated better gene silencing by the guide strand (target complementary strand) and better RNA-induced silencing complex (RISC) assembly[3]. This therapy provides an alternative strategy to treat cancer by silencing the VEGF gene. Angiogenesis is also required for progression and metastasis of melanoma[4], a type of skin cancer that has markedly increased worldwide and caused 80% of skin cancer deaths[5]. Despite a number of strategies have been developed to transfer siRNA/DsiRNA to the target cells, however, the successfulness of its delivery still remains a major difficulty due to rapid degradation by nuclease and macrophages. Therefore, a suitable delivery system is a necessity to protect and deliver it to the target site[6].

Besides protecting the payload, polymeric nanoparticles have other advantages such as ease of synthesis, controllable size and high loading capacity[7]. Chitosan (CS) has attracted much interests as a safe polymeric drug delivery due to biocompatibility and less immunogenic properties which allow it to interact with and protect the carried siRNA/DsiRNA from enzymatic degradation in the cells[8,9]. In dermal and transdermal delivery, pluronic (PF-127) has attracted particular interests because it promotes and improves drug permeation through the skin[10]. The PF-127 is a thermo-reversible gel[11] that exhibits reverse thermal gelation and has low toxicity. At a low concentration (20-30% w/w), it will exist in micellar form while at a high concentration, above the critical gel concentration, it will arrange into lattice form. Thermal gelation properties of PF-127 therefore are able to form depot, lengthen the contact time and prolong the pharmacological action at the desired site[12]. Although, the use of PF-127 as vehicles for various drugs has been previously reported, none has reported on topical application for DsiRNA-loaded CS nanoparticles.

In this study, formulations based on PF-127 were prepared and characterised to serve as a vehicle for DsiRNA-loaded CS nanoparticles into the skin. Nanoparticles loaded with DsiRNA were prepared from water soluble CS for ease of preparation and to reduce risk of cytotoxicity associated with acetic acid residues. The ability of the system to release DsiRNA was later determined using Franz diffusion cell. The safety of this formulation was also assessed in normal cell line *in vitro*.

MATERIALS AND METHODS

Materials: Medium molecular weight CS (Molecular Weight (MW)) of 110-150 kDa with a 75-85% degree of deacetylation (DD) was obtained from Sigma-Aldrich (Ireland), hemicellulase from *Aspergillus niger* was obtained from Sigma-Aldrich (St., Louis, USA), pentasodium tripolyphosphate (TPP) was obtained from Merck (Darmstadt, Germany), DsiRNA targeting the VEGF gene [5'-rGrGrA rGrUrA rCrCrC rUrGrA rUrGrA rGrArU rCrGrA rGrUA C-3' (sense strand) and 5'-rGrUrA rCrUrC rGrArU rCrUrC rArUrC rArGrG rGrUrA rCrUrC rCrCrA-3' (anti-sense strand)] was purchased from Integrated DNA Technologies (IDT), USA. Phosphate Buffered Saline (PBS) was obtained from Sigma-Aldrich (St., Louis, USA), Pluronic, PF-127 powder was purchased from Sigma-Aldrich (St., Louis, MO, USA), while glacial acetic acid with molar mass of 60.05 g mol^{-1} was purchased from R and M Chemicals (United Kingdom). Potassium bromide powder was obtained from Sigma-Aldrich (St., Louis, USA). Cellular acetate membrane with pore size of 0.45 μm was purchased from Sartorius Stedim Biotech (Germany). Chinese hamster lung fibroblasts (V79) cell line was purchased from the American Type Culture Collection (ATCC; Rockville, MD), Dulbecco's Modified Eagle Medium (DMEM) and Fetal Bovine Serum (FBS) were purchased from Sigma-Aldrich (St., Louis, USA). The alamarBlue® was purchased from Invitrogen (Carlsbad, CA, USA) for cell viability assay.

Preparation of water soluble CS: Medium molecular weight CS 1 g was dissolved in 2% v/v glacial acetic acid solution and magnetically stirred (MS MP8 Wise Stir, Wertheim, Germany) at 700 resolution min^{-1} (rpm). The pH of CS solution was adjusted to 4.5 by adding few drops of 1 M NaOH and left overnight. After that, 20% w/v of hemicellulase enzyme solution was added into CS solution and placed in a water bath for 6 h. The pH of CS solution was then adjusted to 5.5 and left overnight. The CS solution was boiled at 100°C for 10 min and superficial layer of the solution containing enzyme was carefully removed. The solution was concentrated to 1/6 of its volume using a rotatory evaporator (Buchi Rotavapour R-200 with Buchi water bath B-480, Chadderton, UK) under a reduced pressure at 60°C and left overnight. Concentrated CS solution was frozen at -80°C and lyophilized (Scanvac Coolsafe Freeze Dryer, Lynge, Denmark) at -110°C for 48 h to form water soluble chitosan.

Structure identification test: A structure identification test was conducted by using a fourier-transform infrared spectrophotometer (FTIR) (Pelkin-Elmer FT-IR 100, Waltham, USA). Three milligrams of sample was mixed with 300 mg of KBr. The sample and KBr powders were ground together in the mortar to produce thoroughly mixed sample. A pressure (Specac Hydraulic Pellet Press, Orpington, USA) of 1 t was applied initially for 1 min and was increased to 10 t for 4 min to form pellets. The FTIR spectra of water soluble and medium weight CS were recorded against the background. For each sample, 16 scans were obtained at a resolution of 4 cm^{-1} in the range of 4000-600 cm^{-1}.

Water solubility test: Water soluble CS obtained was subject to water solubility test. About 0.1 g of sample was dissolved in 10 mL of distilled water at 25°C for 2 h under magnetic stirring (MS MP8 Wise Stir, Wertheim, Germany) at 700 rpm. The CS precipitates were collected by ultracentrifugation (Optima L-100 XP ultracentrifuge, Beckman-Coulter, California, USA) at 10000 rpm for 15 min. The precipitates were placed in an evaporating dish. The precipitates were dried in an oven (Memmert 100 Universal Bench Top Lab Oven, Lund Sweden) until a constant weight was obtained. The evaporating dish was weighed before and after drying. The solubility of water soluble CS was calculated using the following equation:

$$\text{Solubility (\%)} = \frac{\text{Weight of dried CS (g)}}{\text{Initial weight of CS (g)}} \times 100\%$$

Preparation of CS nanoparticles: The CS nanoparticles were prepared using ionic gelation method according to Calvo *et al.*[13] with some modification. The CS solutions (0.1, 0.2 and 0.3% w/v) were prepared by dissolving CS powder in 10 mL distilled water. The TPP solution (0.1% w/v) was prepared by dissolving it in 10 mL distilled water. The CS nanoparticles were produced by adding 1.2 mL of TPP solution drop-wise into 3 mL of CS solutions under a constant magnetic stirring (MS MP8 Wise Stir, Wertheim, Germany) at 700 rpm for 30 min at room temperature. The nanoparticles were later incubated for another 30 min at room temperature before further analysis. The CS nanoparticles were collected by ultracentrifugation twice (Optima L-100 XP ultracentrifuge, Beckman-Coulter, California, USA) at 35,000 rpm and at 10°C for 30 min. The supernatants were discarded and the pellets of nanoparticles were re-suspended in distilled water.

DsiRNA adsorption: The CS nanoparticles were prepared using ionic gelation method prior to DsiRNA adsorption onto the nanoparticles. A volume of 1 mL DsiRNA solution (15 μg mL^{-1}) was added drop-wise to 1 mL of CS nanoparticles suspension made from 0.1, 0.2 and 0.3% w/v CS. The interaction tube was quickly inverted up and down for 10 sec. The particles were then left to incubate for two h at room temperature before further analysis.

Physical characterisation of DsiRNA-loaded CS nanoparticles: Mean particle diameter (Z-average), polydispersity (PdI) and zeta potential (surface charge) of DsiRNA-loaded CS nanoparticles were determined by using a ZS-90 Zetasizer (Malvern Instruments, Worcestershire, UK). No dilution was carried out during the analysis. Each sample was measured in triplicate and the measurements were made at 25°C. The data was reported as Mean±Standard Deviation.

Encapsulation efficiency: The encapsulation efficiency of DsiRNA (%) adsorbed onto the CS nanoparticles was determined from the UV absorption of free DsiRNA in the supernatant recovered from particle centrifugation at 13000×g at 10°C for 15 min using the Allegra 64R centrifuge (Beckman-Coulter, California, USA). The UV absorption of free DsiRNA was determined at the absorbance of 260 nm (λ_{max}). Supernatant recovered from the unloaded CS nanoparticles (without DsiRNA) was used as blank. The concentration of DsiRNA was determined using the Beer's law (A260 = εCL) and calculations were done using the Eq. 1:

$$C = \frac{A}{\varepsilon L} \quad (1)$$

where, C is the concentration of DsiRNA, A260 is the absorbance at 260 nm, ε is the extinction coefficient and L is the path length of the cuvette. The extinction coefficient of DsiRNA is 518500 L mol^{-1} cm^{-1}. After determination of DsiRNA concentration from Eq. 1, the encapsulation efficiency was calculated using the following equation:

$$\frac{C_{sample} - C_{supernatant}}{C_{sample}} \times 100$$

where, C_{sample} is the concentration of DsiRNA added and $C_{supernatant}$ is the concentration of DsiRNA in the supernatant. All the measurements were done in triplicate and the data was reported as Mean±Standard Deviation.

Preparation of pluronic-based gel containing DsiRNA-loaded CS nanoparticles: The PF-127 gels (prepared at concentration of 25 and 30% w/v) were prepared by dissolving PF-127 powder in 3 mL of distilled water at 4°C. The solution was shaken vigorously and allowed to cool at 4°C for 6-8 h. After liquefaction completed, it was stored at 4°C. The CS-DsiRNA nanoparticles was frozen at -20°C and then lyophilised (Scanvac Coolsafe Freeze Dryer, Lynge, Denmark) at -110°C for 48 h. The DsiRNA loaded-CS nanoparticles were incorporated into pluronic by directly mixing them at 4°C for 6 h. The formulations were then stored at 4°C before further analysis.

Characterization of pluronic-based gel containing DsiRNA-loaded CS nanoparticles

Rheological analysis: Rheological analysis was performed using a cone-and-plate rheometer (Bohlin Gemini Rheometer, Worcestershire, UK) with 20 mm diameter and 2° angle system. The shear rate was set to increase from 0-500 sec^{-1} in 3 min followed by a descending shear rate which was back to zero in the same time interval. Three independent measurements were taken for each sample. Average apparent viscosities of each sample were obtained at 500 sec^{-1}.

Scanning electron microscopy: Pluronic gel was frozen at -20°C and then lyophilised (Scanvac Coolsafe Freeze Dryer, Lynge, Denmark) at -110°C for 48 h. Samples were fractured in liquid nitrogen and sputter-coated with gold. The resulting samples were examined using SEM (S-2400, Hitachi, Tokyo, Japan).

Gelation temperature (T_{gel}) measurement: Three millilitres of cold sample solutions were put into a beaker (25 mL) and placed in a low temperature water bath at room temperature. A thermometer was immersed into the sample solution. The solution was heated under continuous magnetic stirring at a constant rate of 200 rpm. The temperature at which the magnetic bar stopped moving was recorded as the gelation temperature.

FTIR spectroscopic analysis: The CS nanoparticles, DsiRNA-CS nanoparticles, blank pluronic gel, DsiRNA-loaded pluronic gel were frozen at -20°C and then lyophilised (Scanvac Coolsafe Freeze Dryer, Lynge, Denmark) at -110°C for 48 h. The KBr pellet method was used in FTIR analysis.

***In vitro* drug release test:** Drug release from the formulations was studied using vertical glass Franz diffusion cells (PermeGear Inc., Hellertown, USA) with a volume of 5.5 mL in a receptor compartment. The diameter of orifice between the donor and receptor was 9 mm with diffusion area of 0.636 cm^2. A Schott bottle containing PBS was maintained at 37°C by placing it in water bath. The whole system was maintained at 37°C. Five millilitres of receptor chamber was filled with PBS until it reached the calibration mark. The uniformity of receptor medium was maintained at a constant rate by stirring using a magnetic bar. Cellulose acetate membrane with a pore size of 0.45 µm (Sterlitech Corporation, Washingtown, USA) was mounted on top of the chamber and equilibrated for 30 min. One gram of the gel was applied onto the membrane. The donor chamber and sampling arm were occluded with parafilm.

Samples (0.5 mL) were withdrawn from the sampling at predetermined time intervals, (30 min, 1, 2, 4, 7, 12, 36, 60, 84, 108, 132 and 156 h). The receptor was replaced with an equal volume of receptor medium in order to maintain sink condition. The amount of released DsiRNA was analysed using a UV-visible spectrophotometer (Shimadzu 1800, Kyoto, Japan) at a wavelength of 260 nm. Capillary cuvette which allows measurement for sample of micro-volume was used. PBS was used as blank solution. The absorbance value of each sample was determined and recorded. The concentration of DsiRNA was determined using Beer's law (A260 = εCL). The cumulative amount of DsiRNA permeated through per surface area (cm^2) of membrane was calculated and plotted against time (h). The rate of drug release from the formulation was determined from the gradient of the plot. In this drug release test, each formulation was run in triplicate.

Cytotoxicity study: The cytotoxicity of gel was evaluated by extraction method recommended by International Organization for Standardization (ISO/EN 10993-5). Lung fibroblast (V79) cell line from the Chinese hamster, procured from ATCC was cultured in DMEM containing FBS (10%) and penicillin-streptomycin (1%). A temperature of 37°C with a humidified 5% CO_2/95% air atmosphere was maintained for the cultures. Cells were seeded in 24 well culture plates (50×10^4 cells $well^{-1}$) and incubated for 24 h. The gel was first incubated in DMEM for 48 h. Subsequently, seeded cells were treated with gel extract for another 24 and 48 h. After incubation at 37°C with gel extract, 20 µL of alamarBlue® reagent was added to the treated cells followed by 4 h incubation prior to analysis. The absorbance of each sample at 570 nm (A570) was measured on a microplate reader. The experiment was performed in triplicates. Cell viability was determined using the following equation:

$$\text{Cell viability (\%)} = \frac{\text{A570 of treated cells}}{\text{A570 of control cells}} \times 100$$

Statistical analysis: Data obtained were presented as Mean±Standard Deviation (SD). The data obtained were analysed with analysis of variance (One-way ANOVA, Tukey *post hoc* analysis) by using SPSS 22.0. The $p<0.05$ indicated statistical significance between the groups tested.

RESULTS AND DISCUSSION

Water soluble CS: Acid-free water soluble CS could be prepared by enzymatic and chemical degradation of CS polymer[14]. The synthesis process through enzymatic reaction is preferable because enzymes can also operate under non-ideal conditions and they are highly specific. Furthermore, the enzymatic degradation minimises alteration in the chemical nature of the product. The broad adsorption band at 3297 cm^{-1} is attributed by the stretching mode of O-H in CS. The adsorption peaks at 2875, 1644 and 1319 cm^{-1} are ascribed to C-H stretching, amide I and -C-O-C- of CS, respectively. Water soluble CS was obtained as indicated by the disappearance of a peak at 1319 cm^{-1} due to the deformation of C-O-C bond as a result of enzymatic action of hemicellulose (Fig. 1). The IR spectrum in previous study showed that there was no significant change in the residues of CS before and after the enzymatic hydrolysis[14]. Assumption of water soluble CS had been successfully synthesised could not be made based on the disappearance of peak of C-O-C bond only. Therefore, solubility test was carried out in this experiment to confirm the successfully synthesis of water soluble CS. In this experiment, the mean solubility of prepared CS was 99.38%. The value was almost 100%, suggesting that the synthesised samples were completely dissolved in water and thereby water soluble CS was successfully synthesised.

Physical characteristics of DsiRNA-loaded CS nanoparticles: A number of studies had reported the physicochemical properties of CS complexes/nanoparticles, including particle size and zeta potential. In general, particle size distribution of CS nanoparticles is in the range of 20-700 nm, depending on the molecular weight of CS used[15,16]. In present study, ionic gelation was used to prepare DsiRNA-CS nanoparticles. In this method, nanoparticles are produced by electrostatic interaction and ionotropic gelation between CS and TPP polyanion[17,18] and it requires a mild preparation condition e.g., temperature and pH[19].

Particle size influences the amount of drug loading, drug release and stability of nanoparticles[20]. In this study, concentration of TPP had been optimised and fixed, whereby different concentrations of CS were used to determine its effect on the particle size. According to Katas *et al.*[21], the particle size of CS nanoparticles increases as the concentration of CS is increased. Similar to that, the mean particle size of CS nanoparticles (Table 1) increased significantly from 170±13.3 to 283±6.2 nm with increasing of CS concentration from 0.1-0.3% w/v ($p<0.05$, ANOVA, Turkey *post hoc* analysis). At lower concentrations, CS has a better ability to contact with polyanions and form inter and intra-molecular linkages due to higher solubility. Nanoparticles are formed immediately upon mixing of TPP and CS solutions as molecular linkages are formed between TPP phosphates and CS amino groups, thus resulting in smaller particle size[21].

The DsiRNA was loaded to CS nanoparticles by adsorption method according to a previous study[22]. The mean particle size of unloaded CS nanoparticles was larger than DsiRNA-loaded CS nanoparticles. This could be explained by the fact that negative charge of DsiRNA neutralised the positive charge of CS, resulting in a smaller particle size as the conformation of CS molecule became less extended or more compact[21]. In addition to that, the mean particle size of CS-DsiRNA nanoparticles was also significantly increased with the increase in CS concentration ($p<0.05$, ANOVA, Turkey *post hoc* analysis). At higher concentrations of CS, it is expected that higher electrostatic repulsion exhibited by CS molecules would subsequently make the CS molecules became less able to contact with polyanion (TPP), thus resulting in larger size of individual particle. Moreover, CS-DsiRNA nanoparticles prepared from various CS concentrations had PdI values lower than 0.5, indicating the particles were narrowly distributed.

Table 1: Physical characteristic CS-DsiRNA nanoparticles, n = 3

	Mean particle size (nm)±SD		PdI±SD		Zeta potential (mV)±SD		EE (%)±SD
CS (% w/v)	Blank	Loaded	Blank	Loaded	Blank	Loaded	Loaded
0.1	170.8±13.3	146.0±19.3	0.32±0.06	0.41±0.06	-1.6±1.0	-2.3±0.8	90.1±1.8
0.2	238.4±17.5	217.7±20.5	0.32±0.02	0.41±0.02	+33.6±2.3	+31.7±0.7	81.8±1.8
0.3	283.3±6.2	266.3±14.1	0.39±0.04	0.42±0.03	+44.3±0.9	+40.6±1.6	69.9±1.4

EE: Encapsulation efficiency

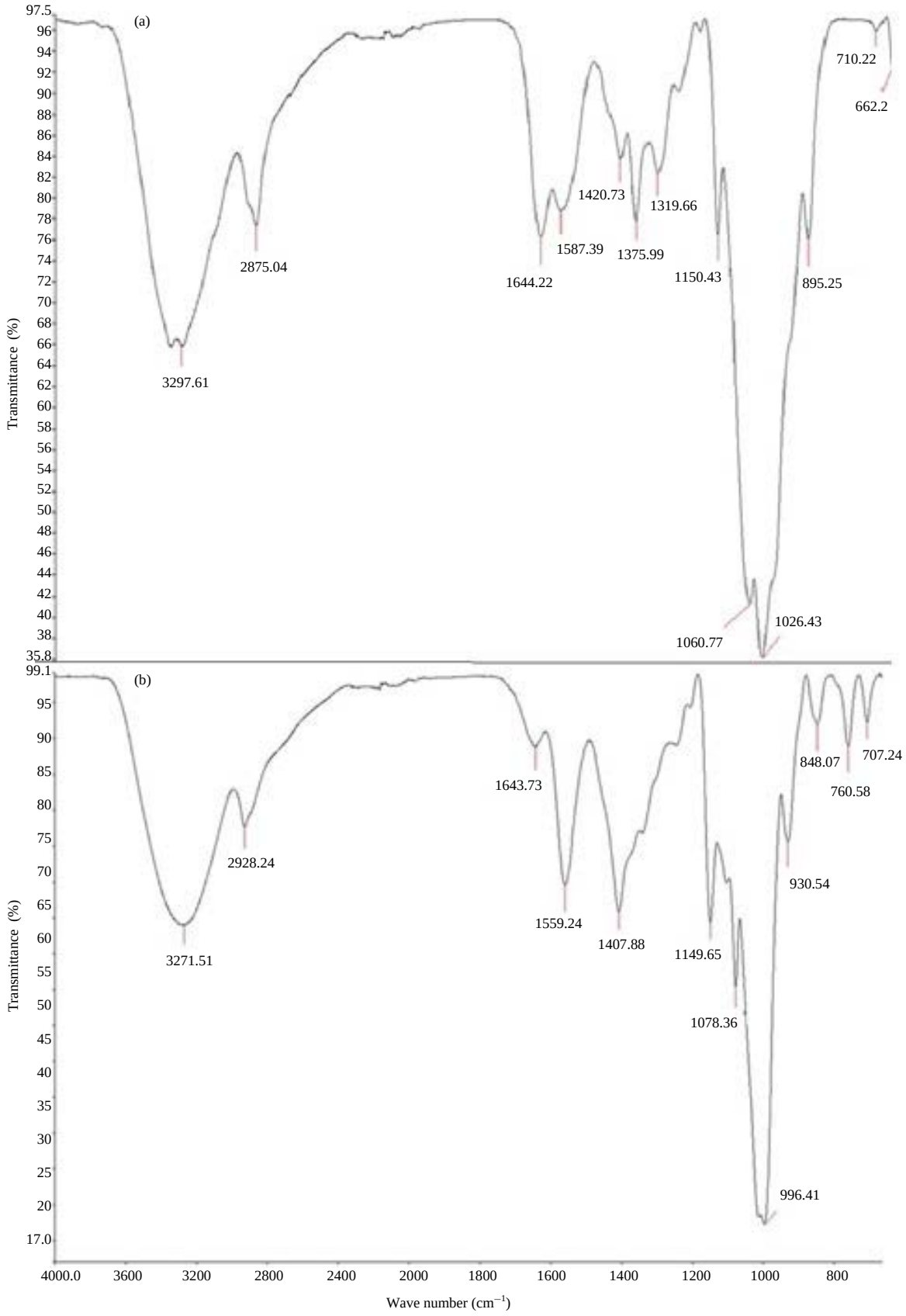

Fig. 1(a-b): FTIR spectrum of medium (a) Molecular weight CS and (b) Water soluble CS

Surface charge is characterised by zeta potential[23]. A net positive charge is important for successful transfection in gene delivery studies[8]. The zeta potential of unloaded CS nanoparticles (Table 1) increased significantly when the concentration of CS was increased ($p<0.05$, ANOVA, Turkey *post hoc* analysis). The increased zeta potential was attributed by increased excess CS positive charges which were not counteracted with the negatively charged TPP ions. Loading of DsiRNA onto the CS nanoparticles had significantly reduced their zeta potential. The presence of phosphate groups of DsiRNA would compensate for the positive charges of CS and thus, reducing its zeta potential. All formulations had positive surface charges except for CS-DsiRNA nanoparticles prepared from the lowest CS concentration (0.1% w/v), attributed by an excessive negative charge from DsiRNA. At higher CS concentrations (0.2, 0.3% w/v), CS-DsiRNA nanoparticles had a net positive charge as the density of positive charges was higher that the negative charges which resulted in an excessive of CS positive charges[24]. This also explained the finding that zeta potential of CS-DsiRNA nanoparticles increased significantly as the concentration of CS was increased from 0.2-0.3% w/v ($p<0.05$, independent t-test). Nanoparticles with a net positive charge were advantageous for stability of the system as formation of aggregation could be minimised[25].

High encapsulation efficiency is vital for an effective drug delivery system[20] and it is related to the polymer composition, molecular weight and drug-polymer interaction[26]. From this experiment, the encapsulation efficiency decreased significantly ($p<0.05$, ANOVA, Tukey *post hoc* analysis) when the CS concentration was increased (Table 1). The encapsulation efficiency decreased from 90.1 ± 1.8 to 69.9 ± 1.4% when the CS concentration was increased from 0.1-0.3% w/v which expected to be due to the increased of CS viscosity. The higher viscosity restrains the encapsulation of DsiRNA by hindering the movement of DsiRNA around the CS chain as proposed by Vandenberg *et al.*[27]. Apart from viscosity, CS concentration is expected to indirectly affect the encapsulation efficiency of such system by influencing particle size. The larger particle size of CS nanoparticles (as the CS concentration increased) would have smaller surface area available for DsiRNA adsorption process. Thus, adsorption ability of CS nanoparticles would be reduced with higher concentration of CS[28].

Rheology and morphology of gel: Rheology of the formulation was analysed to obtain information on the stability and performance of products[29]. The viscosity of formulation is important as it is the property that enables adhesive to flow into adherent and attach firmly. Many studies have been done to focus on the effects of additives on the rheological behaviour and thermo-sensitivity of PF-127. According to Varshosaz *et al.*[30], a combination of CS/poloxamer gel exhibited pseudoplastic flow in non-physiological condition. In present study, it was observed that pluronic had different apparent viscosities even at the same concentration when different CS nanoparticles were added (prepared from different concentrations of CS) (Fig. 2). In case of 25% w/v PF-127, the mean apparent viscosity of CS nanoparticles prepared from 0.2% w/v CS concentration was increased to 0.839 ± 0.04 Pa sec as compared to 0.751 ± 0.005 Pa sec for 0.1% w/v. Meanwhile for 30% w/v PF-127, the mean apparent viscosity increased from 1.181 ± 0.577 to 1.212 ± 0.189 Pa sec. This could be explained by the fact that when CS was added into a solvent, the solvent gradually diffused into CS polymer and resulted in swelling of the polymer. Swelled CS molecules would impede the flow of any molecule in the pluronic gel and thus, impart on the viscosity[31]. A shift to the right of the graph was observed when 30% w/v of PF-127 was used. This was expected as more entanglement would occur at high PF-127 concentration to produce micelles. As a result, PF-127 molecules could not be separated easily from one another, which accounted for the rigidity and high viscosity of gel containing high concentration of pluronic[32].

Morphology is important for colloidal and chemical stability besides bioactivity of nanoparticles[32]. In this study, the morphology of DsiRNA-loaded CS nanoparticles and pluronic gels were investigated using SEM. The SEM was used to visualise the surface of pluronic gels containing DsiRNA-loaded CS nanoparticles. In this study, under the magnification between 2000 and 2500x, some pores among the fibrous structures of pluronic gels could be observed. The SEM images of pluronic gels showed an irregular texture with different pore size[33]. Besides, the presence of DsiRNA-loaded CS nanoparticles on the surface of pluronic gel could be seen. The morphology of DsiRNA-loaded CS nanoparticles could be clearly examined when higher magnifications were applied (between 10000-150000x). Figure 3 shows DsiRNA-loaded CS nanoparticles present in the pluronic gels. According to Katas *et al.*[22] DsiRNA-loaded CS nanoparticles showed spherical morphology. Figure 3 showed that DsiRNA-loaded CS nanoparticle mostly had spherical shape, with some irregular nanoparticles. As the CS concentration increased, the nanoparticles became more irregular in shape and poly-dispersed. Some degree of aggregation could also be seen from the images which coincided with the finding of particle polydispersity. Aggregation of small nanoparticles could occur as they tend to fuse together and forming bigger particles in order to reduce their surface energy[34].

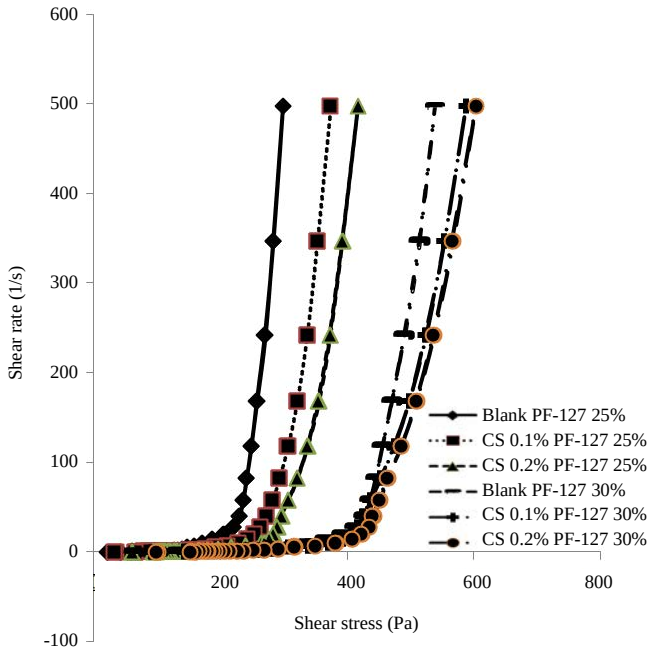

Fig. 2: Rheological behaviour of pluronic gels containing CS-DsiRNA nanoparticles, n = 3

Table 2: Gelation temperature (T_{gel}) of CS-DsiRNA nanoparticles, n = 3

Formulation	T_{gel}±SD
0.1% CS+25% PF-127	24.3±0.6
0.2% CS+25% PF-127	25.3±0.6
0.1% CS+30% PF-127	20.7±0.6
0.2% CS+30% PF-127	21.3±0.6

T_{gel} and FTIR spectroscopic analysis: The T_{gel} is the temperature which the liquid phase makes a transition into gel. At low temperature, PF-127 molecules are surrounded by hydration layer. But, when the temperature was increasing, breakage of the hydrogen bond occurred between the water molecule and the hydrophilic chain of PF-127 tended to more favour towards hydrophobic interaction between polyoxypropylene domain and led to gel formation[12]. The T_{gel} for topical thermo-reversible gel is suitable if it is within the range of 25-37°C. If T_{gel}<25°C, a gel might be formed at room temperature, leading to difficulty in manufacturing, handling[35] and cannot apply onto the skin to form a solid artificial barrier and sustained release depot[12]. In this study, T_{gel} of pluronic was remained unchanged regardless of CS concentration used to prepare nanoparticles (Table 2). This could be due to the high proportion of pluronic to CS ratio in the gel and therefore, T_{gel} mostly depends on the hydrophobic interaction between polyoxpropylene. In contrast to that, a significant difference in T_{gel} was observed when pluronic concentration was increased ($p<0.05$, independent t-test). At high concentration of pluronic, the solution consisted more micelles and the micelles were likely to bind less water molecules and easily aggregate to form gel. Thus, the T_{gel} became lower compared to a low pluronic concentration[36].

Absorption band could be seen in the IR spectra and resulted from the bond vibration. Polymer and drug have their own spectra. Loading of drug into polymer will produce a different spectrum which can be used to determine whether the drug has been successfully incorporated into the system[37]. In this study, spectrum of unloaded CS nanoparticles (prepared from 0.2% w/v CS concentration), CS-DsiRNA nanoparticles, blank pluronic gel and DsiRNA-loaded pluronic gel were obtained to determine successful incorporation of CS-DsiRNA nanoparticles within the pluronic gel. The FTIR spectra are presented in Fig. 4. The spectrum of unloaded CS nanoparticles shows characteristic peaks of CS at 3413 cm^{-1} (-OH stretching), 2927 cm^{-1} (-CH stretching) and 1092.62 cm^{-1} (C-O-C stretching) while TPP at 895 cm^{-1}. In the spectrum of CS-DsiRNA nanoparticles, characteristic of DsiRNA (P-CH_3) and (P-CH_2) bending peaks are seen at 1555 and 1648.18 cm^{-1}, respectively. Moreover, P=O stretching could be observed in the region of 1270 cm^{-1}. The bands of pluronic (unloaded/empty gel) could be seen in the spectral region of 3445, 2888 and 1112 cm^{-1} which correspond to the stretching vibrations of OH, CH and C-O groups, respectively. The spectrum of DsiRNA-loaded pluronic gel shows the light shift of characteristic peaks of pluronic. However, the absence of characteristic peaks of CS, TPP, DsiRNA in pluronic gel indicates the successful incorporation of the nanoparticulate system into the gel or the nanoparticles are located within the gel as similar finding was reported elsewhere[38].

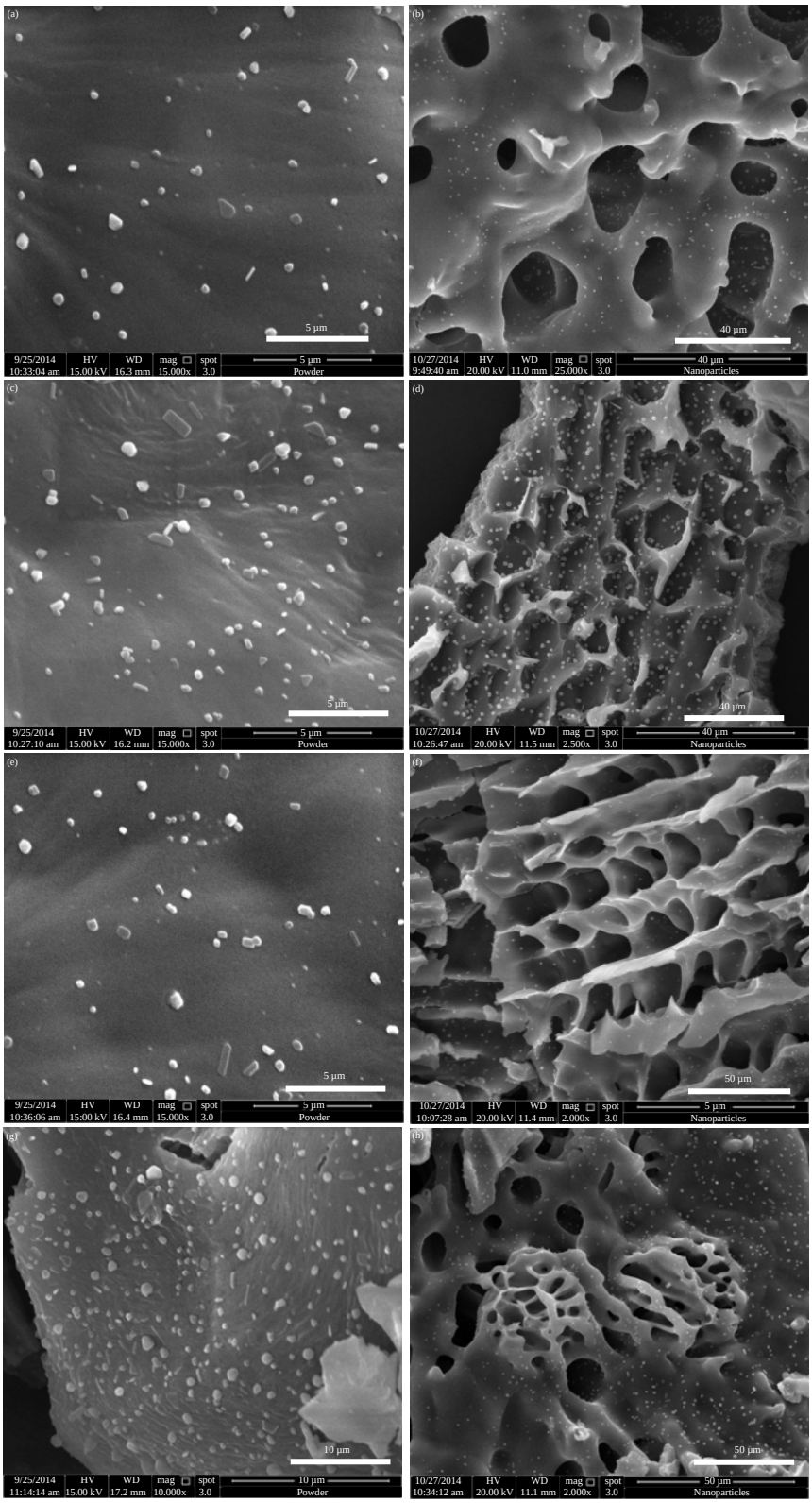

Fig. 3(a-h): SEM images of DsiRNA-loaded CS nanoparticles incorporated into pluronic gel, (a and b) 0.1% CS+25% PF-127, (c and d) 0.2% CS+25% PF-127, (e and f) 0.1% CS+30% PF-127 and (g and h) 0.2% CS+30% PF-127, images on the left are of higher magnification (10000-15000x), whereas the images on the right are of lower magnification (2000-2500x)

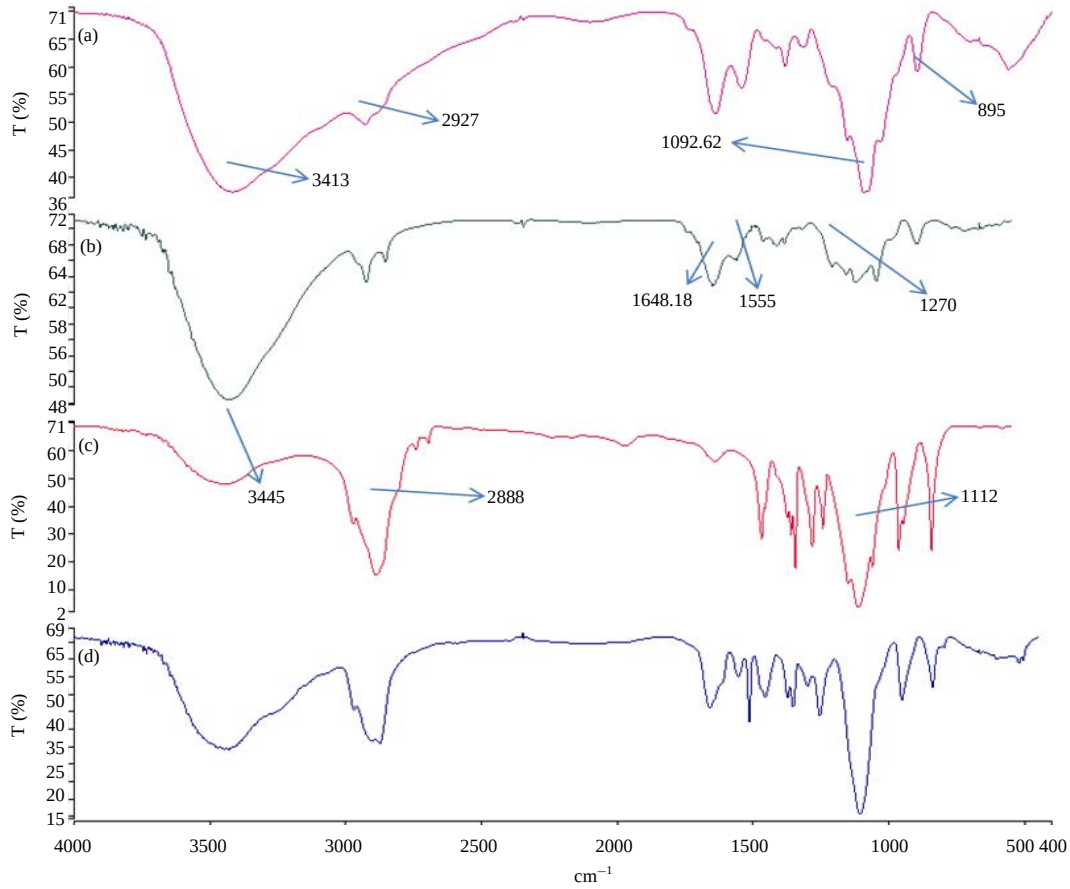

Fig. 4(a-d): FTIR spectra of 0.2% w/v CS: (a) Unloaded CS nanoparticles, (b) CS-DsiRNA nanoparticles, (c) Blank pluronic gel and (d) CS-DsiRNA nanoparticles-loaded pluronic gel

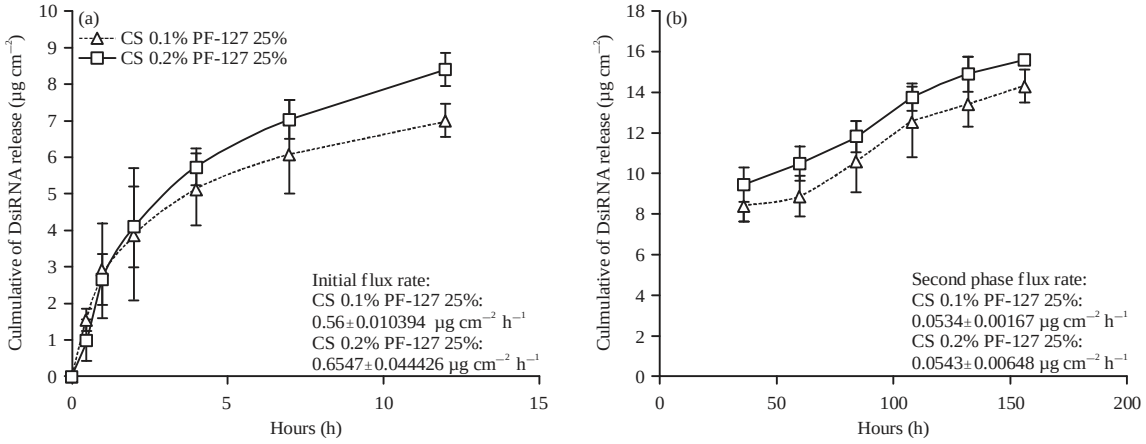

Fig. 5(a-b): *In vitro* drug release profile of CS-DsiRNA nanoparticles at (a) First stage (first 12 h) and (b) Phase 2 (after 12 h), n = 3

***In vitro* drug release test:** The drug release profile of DsiRNA from the CS nanoparticles in pluronic gel was determined by using Franz diffusion cells (Fig. 5). The study was carried out for 7 days and the system was maintained at pH 7.4. Cumulative release in percentage was calculated based on the amount of DsiRNA released into the releasing medium. CS nanoparticles prepared from 0.1 and 0.2% w/v CS concentrations were selected due to their high entrapment

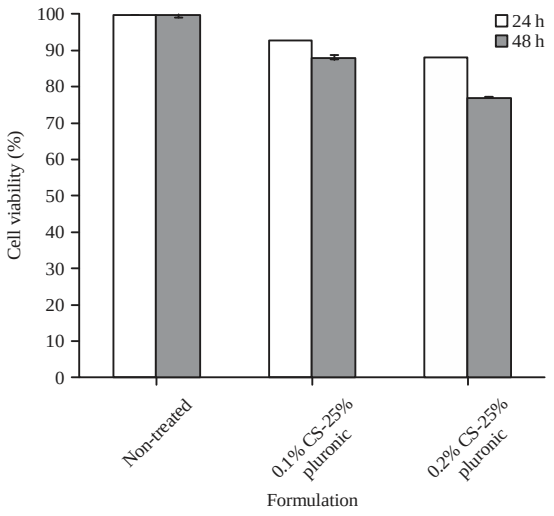

Fig. 6: Cytotoxicity effect of gels containing CS-DsiRNA nanoparticles, n = 3

efficiencies. The nanoparticles were later incorporated into a gel formulation containing 25% w/v pluronic due to its gelation temperature within the range of 25-37°C. Figure 5 illustrates the release of DsiRNA from the particles in the gel. The DsiRNA-loaded CS nanoparticles prepared from 0.1 and 0.2% w/v CS concentrations initially showed a rapid release of 39.86±2.647 and 43.36±2.347% of the loaded amount, respectively. The rapid release lasted for 12 h. The release of DsiRNA from CS nanoparticles is observed to be dependent on the encapsulation efficiency. The CS nanoparticles with low encapsulation efficiency released more DsiRNA into the releasing medium because intermolecular linkages between DsiRNA and CS were expected to be weaker. In the second stage, DsiRNA was released at a constant rate (sustained release) from CS nanoparticles up to 6 days. The total amounts of cumulative DsiRNA released after 6 days were 81.49 and 80.39% of the loaded amount for CS nanoparticles prepared from 0.1 and 0.2% w/v, respectively.

The obtained flux rates in this study could be categorised into two stages. At the first stage, the mean flux rate for DsiRNA-loaded CS nanoparticles prepared from 0.1 and 0.2% w/v were 0.5086±0.0103 and 0.6547±0.0444 μg cm^{-2} h^{-1}, respectively. Statistical analysis proved that the flux rate for these two formulations were significant different from one another ($p<0.05$, independent t-test). The CS nanoparticles with low entrapment efficiency released DsiRNA faster to the releasing medium because the interaction between DsiRNA and CS might be weaker as mentioned above[39]. Meanwhile, at the second stage, the mean flux rate for DsiRNA-loaded CS nanoparticles prepared from 0.1 and 0.2% w/v were 0.0534±0.002 and 0.0543±0.007 μg cm^{-2}, respectively. Unlike the first stage, the mean flux rate between these two formulations was not significantly different. This phenomenon could be attributed by the presence of remaining DsiRNA which was tightly bound to CS nanoparticles that had been slowly released at a constant rate to the releasing medium.

Cytotoxicity: In this experiment, cytotoxicity study was carried out with the aim to assess the safety of this formulation in normal cells. Figure 6 shows that cell viability was 88-93% when treated with the gels containing CS-DsiRNA nanoparticles at 24 h. Lower cell viability was measured for formulation containing CS-DsiRNA nanoparticles prepared from 0.2% w/v CS. On the other hand, an average of 12-23% loss in cell viability was observed for gels containing CS-DsiRNA nanoparticles at 48 h. Similar to the cell viability at 24 h, CS nanoparticles prepared from higher CS concentration caused a greater cell loss. No significant difference was observed in the cytotoxicity between the gels and non-treated cell (control) except for the gel containing CS-DsiRNA nanoparticles prepared from 0.2% w/v CS at 48 h. The loss of cell viability might be due to leaching of more un-reacted CS from the gel and the effect was more prominent when exposed for a longer period of time. Further investigation in different cell lines is therefore needed to address this effect.

CONCLUSION

High encapsulation efficiency of DsiRNA-loaded CS nanoparticles were successfully prepared using ionic gelation method and they were successfully incorporated into thermo-sensitive gel formulation by using 25% w/v pluronic. The formulated pluronic gel had the desirable viscosity and T_{gel}. These formulations were relatively safe to the cells and exhibited sustained DsiRNA release which showed promising application in topical delivery. Further investigation on the stability, *in vitro* and *in vivo* efficacy of the system are necessary to optimise the delivery of DsiRNA to the target cells and ultimately, to produce gene silencing effect of VEGF.

ACKNOWLEDGMENT

The authors gratefully acknowledge the financial support provided by the Universiti Kebangsaan Malaysia and Ministry of Education of Malaysia (FRGS/1/2015/SKK09/UKM/02/1).

REFERENCES

1. Hanahan, D. and R.A. Weinberg, 2011. Hallmarks of cancer: The next generation. Cell, 144: 646-674.
2. Zhan, P., J. Wang, X.J. Lv, Q. Wang and L.X. Qiu *et al*., 2009. Prognostic value of vascular endothelial growth factor expression in patients with lung cancer: A systematic review with meta-analysis. J. Thoracic Oncol., 4: 1094-1103.
3. Snead, N.M., X. Wu, A. Li, Q. Cui, K. Sakurai, J.C. Burnett and J.J. Rossi, 2013. Molecular basis for improved gene silencing by dicer substrate interfering Rna compared with other siRNA variants. Nucleic Acids Res., 41: 6209-6221.
4. Mehnert, J.M., M.M. McCarthy, L. Jilaveanu, K.T. Flaherty and S. Aziz *et al*., 2010. Quantitative expression of VEGF, VEGF-R1, VEGF-R2 and VEGF-R3 in melanoma tissue microarrays. Hum. Pathol., 41: 375-384.
5. Paluncic, J., Z. Kovacevic, P.J. Jansson, D. Kalinowski and A.M. Merlot *et al*., 2016. Roads to melanoma: Key pathways and emerging players in melanoma progression and oncogenic signaling. Biochimica et Biophysica Acta (BBA)-Mol. Cell Res., 1863: 770-784.
6. Katas, H., N.N.S.N. Dzulkefli and S. Sahudin, 2012. Synthesis of a new potential conjugated TAT-peptide-chitosan nanoparticles carrier via disulphide linkage. J. Nanomater., Vol. 2012. 10.1155/2012/134607.
7. Li, S.D. and L. Huang, 2007. Non-viral is superior to viral gene delivery. J. Controlled Release, 123: 181-183.
8. Csaba, N., M. Koping-Hoggard and M.J. Alonso, 2009. Ionically crosslinked chitosan/tripolyphosphate nanoparticles for oligonucleotide and plasmid DNA delivery. Int. J. Pharm., 382: 205-214.
9. Mao, S., W. Sun and T. Kissel, 2010. Chitosan-based formulations for delivery of DNA and siRNA. Adv. Drug Delivery Rev., 62: 12-27.
10. He, P., S.S. Davis and L. Illum, 1998. *In vitro* evaluation of the mucoadhesive properties of chitosan microspheres. Int. J. Pharma., 166: 75-88.
11. Kim, S.Y., J.C. Ha and Y.M. Lee, 2000. Poly(ethylene oxide)-poly(propylene oxide)-poly(ethylene oxide)/poly(ϵ-caprolactone) (PCL) amphiphilic block copolymeric nanospheres: II. Thermo-responsive drug release behaviors. J. Controlled Release, 65: 345-358.
12. Escobar-Chavez, J.J., M. Lopez-Cervantes, A. Naik, Y. Kalia, D. Quintanar-Guerrero and A. Ganem-Quintanar, 2006. Applications of thermo-reversible pluronic F-127 gels in pharmaceutical formulations. J. Pharma. Pharma. Sci., 9: 339-358.
13. Calvo, P., C. Remunan-Lopez, J.L. Vila-Jato and M.J. Alonso, 1997. Novel hydrophilic chitosan-polyethylene oxide nanoparticles as protein carriers. J. Applied Polym. Sci., 63: 125-132.
14. Qin, C., Y. Du, L. Zong, F. Zeng, Y. Liu and B. Zhou, 2003. Effect of hemicellulase on the molecular weight and structure of chitosan. Polymer Degrad. Stabil., 80: 435-441.
15. Fernandez-Urrusuno, R., P. Calvo, C. Remunan-Lopez, J.L. Vila-Jato and M.J. Alonso, 1999. Enhancement of nasal absorption of insulin using chitosan nanoparticles. Pharm. Res., 16: 1576-1581.
16. Pan, Y., Y.J. Li, H.Y. Zhao, J.M. Zheng and H. Xu *et al*., 2002. Bioadhesive polysaccharide in protein delivery system: Chitosan nanoparticles improve the intestinal absorption of insulin *in vivo*. Int. J. Pharm., 249: 139-147.
17. Dyer, A.M., M. Hinchcliffe, P. Watts, J. Castile and I. Jabbal-Gill *et al*., 2002. Nasal delivery of insulin using novel chitosan based formulations: A comparative study in two animal models between simple chitosan formulations and chitosan nanoparticles. Pharm. Res., 19: 998-1008.
18. Janes, K.A., P. Calvo and M.J. Alonso, 2001. Polysaccharide colloidal particles as delivery systems for macromolecules. Adv. Drug Delivery Rev., 47: 83-97.
19. Zhang, H., M. Oh, C. Allen and E. Kumacheva, 2004. Monodisperse chitosan nanoparticles for mucosal drug delivery. Biomacromolecules, 5: 2461-2468.
20. Mohanraj, V.J. and Y. Chen, 2006. Nanoparticles: A review. Trop. J. Pharma. Res., 5: 561-573.
21. Katas, H., M.A.G. Raja and K.K. Lam, 2013. Development of chitosan nanoparticles as a stable drug delivery system for protein/siRNA. Int. J. Biomat. 10.1155/2013/146320
22. Katas, H., M.A.G. Raja, Z.A. Hamid and N.A. Razali, 2013. Physicochemical properties and *in vitro* cytotoxicity studies of chitosan as a potential carrier for dicer-substrate siRNA. J. Nanomat. 10.1155/2013/653892.
23. Couvreur, P., G. Barratt, E. Fattal, P. Legrand and C. Vauthier, 2002. Nanocapsule technology: A review. Crit. Rev. Ther. Drug Carrier Syst., 19: 99-134.
24. Hejazi, R. and M. Amiji, 2003. Chitosan-based gastrointestinal delivery systems. J. Control Release, 89: 151-165.
25. Schiffelers, R.M., M.C. Woodle and P. Scaria, 2004. Pharmaceutical prospects for RNA interference. Pharm. Res., 21: 1-7.
26. Govender, T., S. Stolnik, M.C. Garnett, L. Illum and S.S. Davis, 1999. PLGA nanoparticles prepared by nanoprecipitation: Drug loading and release studies of a water soluble drug. J. Controlled Release, 57: 171-185.
27. Vandenberg, G.W., C. Drolet, S.L. Scott and J. de la Noue, 2001. Factors affecting protein release from alginate-chitosan coacervate microcapsules during production and gastric/intestinal simulation. J. Controlled Relase, 77: 297-307.
28. Sugita, P., L. Ambarsari and F. Farichah, 2013. Increasing amount and entrapment efficiency of chitosan-ketoprofen nanoparticle using utrasonication method with varied time and amplitude. Int. J. Res. Rev. Applied Sci., 14: 612-618.

29. Almeida, I.F. and M.F. Bahia, 2006. Evaluation of the physical stability of two oleogels. Int. J. Pharm., 327: 73-77.
30. Varshosaz, J., M. Tabbakhian and Z. Salmani, 2008. Designing of a thermosensitive chitosan/poloxamer in situ gel for ocular delivery of ciprofloxacin. Open Drug Deliv. J., 2: 61-70.
31. Chattopadhyay, D.P. and M.S. Inamdar, 2010. Aqueous behaviour of chitosan. Int. J. Polym. Sci., Vol. 2010. 10.1155/2010/939536.
32. Ibrahim, E.S., S. Ismail, G. Fetih, O. Shaaban, K. Hassanein and N. Abdellah, 2012. Development and characterization of thermosensitive pluronic-based metronidazole *in situ* gelling formulations for vaginal application. Acta Pharma., 62: 59-70.
33. Chen, C.C., C.L. Fang, S.A. Al-Suwayeh, Y.L. Leu and J.Y. Fang, 2011. Transdermal delivery of selegiline from alginate-Pluronic composite thermogels. Int. J. Pharm., 415: 119-128.
34. Rampino, A., M. Borgogna, P. Blasi, B. Bellich and A. Cesaro, 2013. Chitosan nanoparticles: Preparation, size evolution and stability. Int. J. Pharm., 455: 219-228.
35. Meenakshi, P., T. Hetal and P.V. Kasture, 2010. Preparation and evaluation of thermoreversible formulations of flunarizine hydrochloride for nasal delivery. Int. J. Pharm. Pharm. Sci., 2: 115-120.
36. Bromberg, L.E. and E.S. Ron, 1998. Temperature-responsive gels and thermogelling polymer matrices for protein and peptide delivery. Adv. Drug Deliv. Rev., 31: 197-221.
37. Jaya, S., T.D. Durance and R. Wang, 2010. Physical characterization of drug loaded microcapsules and controlled *in vitro* release study. Open Biomat. J., 5: 9-17.
38. Zhang, W., Y. Shi, Y. Chen, J. Hao, X. Sha and X. Fang, 2011. The potential of Pluronic polymeric micelles encapsulated with paclitaxel for the treatment of melanoma using subcutaneous and pulmonary metastatic mice models. Biomaterials, 32: 5934-5944.
39. Mehta, R.C., B.C. Thanoo and P.P. DeLuca, 1996. Peptide containing microspheres from low molecular weight and hydrophilic poly (D,L-lactide-co-glycolide). J. Controlled Rel., 41: 249-257.